Available online at www.sciencedirect.com
SCIENCE DIRECT
ELSEVIER
Coordination Chemistry Reviews 249 (2005) 2642–2648
COORDINATION CHEMISTRY REVIEWS
www.elsevier.com/locate/ccr

Review

Magnetism of metal cyanide networks assembled at interfaces

Jeffrey T. Culp [a], Ju-Hyun Park [b], Franz Frye [a], Young-Duk Huh [a,1], Mark W. Meisel [b,*], Daniel R. Talham [a,*]

[a] *Department of Chemistry, University of Florida, P.O. Box 117200, Gainesville, FL 32611-7200, USA*
[b] *Department of Physics and Center for Condensed Matter Sciences, University of Florida, Gainesville, FL 32611-8440, USA*

Received 2 February 2005
Available online 11 July 2005

Contents

Abstract

Studies of metal cyanide thin films prepared directly at interfaces are reviewed. The systems range from monolayers, single-layer analogs of Prussian blue-like networks, to bulk powders prepared as thin films. Monolayer networks are prepared at the air/water interface and transferred to solid supports using Langmuir–Blodgett film methods. Films of bulk materials are prepared directly on solid surfaces using a templated sequential deposition procedure. The magnetic properties of the films have been explored, and in some cases, these monolayers and surface films give rise to new behavior that is only possible because of the fabrication method or thin film architecture. The methods of synthesis can generate oriented samples, even when the materials are poorly crystalline. Furthermore, the interface-assembled networks are inherently anisotropic, leading to phenomena not present in the solid-state analogs, such as anisotropic photomagnetism in a thin film of $Rb_jCo_k[Fe(CN)_6]_l{\cdot}nH_2O$.

Keywords: Photoinduced magnetism; Supramolecular; Cyanometallates; Monolayers; Thin films; Molecule-based magnets; Prussian blue analog

1. Introduction

Despite impressive advances in supramolecular synthesis, many of the promised technological applications of the new nano structures will still require positioning structures at interfaces. An attractive alternative to the multistep process of synthesis–isolation–deposition, is to fabricate nanoscale objects at the site of use, providing motivation to investigate supramolecular assembly directly at a surface or interface. These ideas are particularly relevant in the area of molecule-based magnets, for which the structure-directing properties of coordinate covalent bonds have been exploited for the supramolecular design of beautiful molecular and network magnetic structures, and applications

* Corresponding authors.
E-mail addresses: meisel@phys.ufl.edu (M.W. Meisel), talham@chem.ufl.edu (D.R. Talham).
[1] Permanent address: Department of Chemistry, Dankook University, Seoul, Korea.

0010-8545/$ – see front matter © 2005 Elsevier B.V. All rights reserved.
doi:10.1016/j.ccr.2005.05.011

such as information storage require a surface or solid support.

Metal cyanide extended networks, analogs of Prussian blue, have been of keen interest to the molecule-based magnetism community [1–3], because the nature of the magnetic exchange can be anticipated in advance from basic orbital interaction arguments and the predictable structure-directing quality of the cyanide bridge facilitates supramolecular and network design [4]. The cubic Prussian blue analogs have the general formula $M_jA_k[B(CN)_6]_l{\cdot}nH_2O$ where A and B can be divalent or trivalent transition metals in ratios that depend on the relative charges of the metal ions and the number of vacancies in the structure. Charge balancing monovalent cations, M, may also be present. Many lower dimensional extended networks are also known. A wide range of magnetic phenomena have been observed in metal cyanides, including high-spin clusters [5–10], metamagnetism [4,11–13], room temperature magnetic ordering [14–16], spin-glass behavior [17,18], and photomagnetism [19–21].

The inherent ability to tailor both the structure and magnetic exchange in metal-cyanide systems also makes this family of materials well suited for exploring supramolecular assembly at interfaces. This review will highlight some of our group's recent studies of metal cyanide thin films prepared directly at interfaces. The systems range from monolayers, single-layer analogs of Prussian blue-like networks, to bulk powders prepared as thin films. The magnetic properties of the films have been explored. In some cases, these monolayers and surface films give rise to new behavior that is only possible because of our method of fabrication. For example, the method of synthesis generates oriented samples, even when the materials are poorly crystalline. Furthermore, the interface-assembled networks are inherently anisotropic, even if the parent structure is cubic, leading to phenomena not present in the solid-state analogs.

2. Cyanometallate monolayers

To prepare monolayers, networks can be synthesized at the air/water interface [22,23]. The surface of water retains the structure-directing property of an interface but at the same time is fluidic, enabling diffusion of reactants. The water surface is also flat, which facilitates some characterization methods including Brewster angle microscopy and grazing incidence X-ray diffraction (GIXD) [22,23].

Our approach for assembly at an interface is outlined in Fig. 1. The target in this example is a square grid nickel–iron–cyanide network that arises from the 90° bond angles around the starting iron cyanide complex, **1**. The product is a single monolayer of a two-dimensional square grid because the amphiphilic dialkylaminopyridine ligand confines the iron complex to the interface, thereby directing the condensation reaction within the plane of the water surface. In the absence of the interface, the pentacyanoferrate(3+) starting complex is capable of forming bridges that lead to geometries other than a square grid, and when the reaction is carried out in solution, only amorphous products are observed [22]. The interface facilitates bridging in the equatorial plane of the amphiphilic complex, and therefore plays an important role in controlling the final structure. Monolayer networks based on **1** with Co^{2+} or Mn^{2+} in place of Ni^{2+} have also been prepared [23].

The two-dimensional grid networks depicted in Fig. 1, have been structurally characterized by grazing incidence X-ray diffraction, and chemically characterized with X-ray

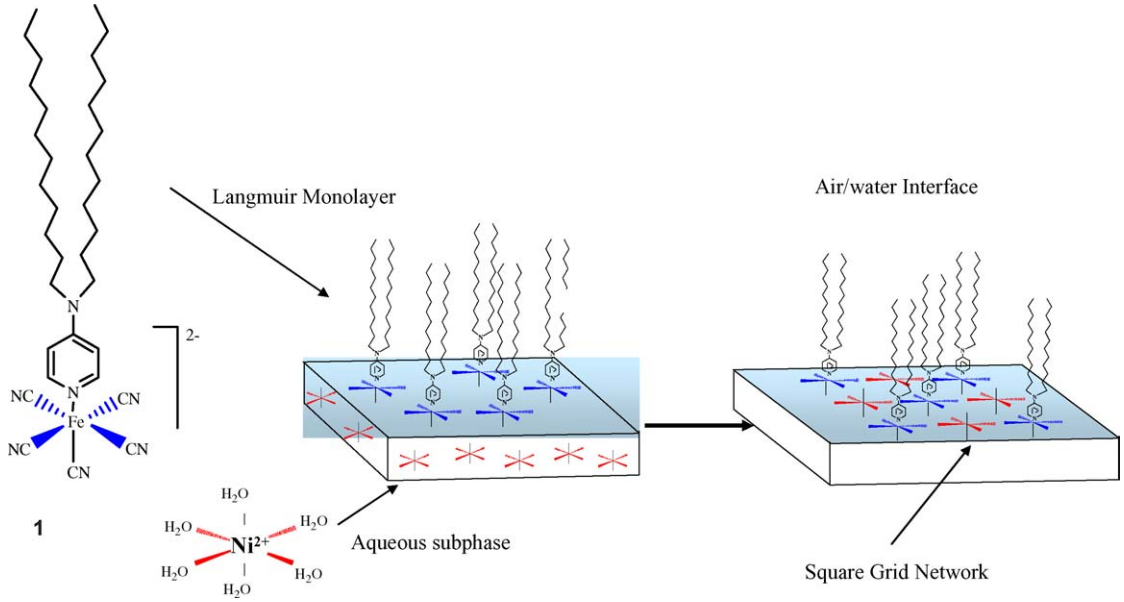

Fig. 1. Reaction of an amphiphilic pentacyanoferrate complex, **1**, confined to the air/water interface, with aqueous metal ions results in a mixed-metal cyanide bridged square grid network. In addition to the Ni^{2+} example, shown, square grid monolayer networks have been formed with Co^{2+} and Mn^{2+}.

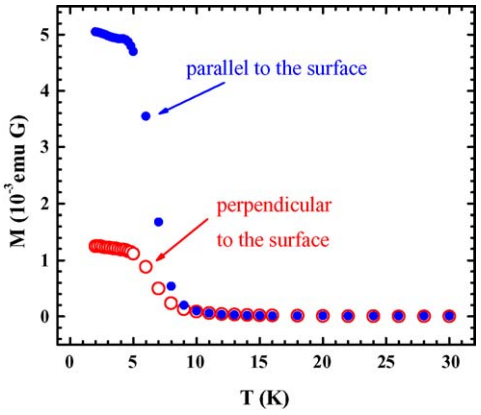

Fig. 2. Field cooled magnetization vs. temperature for a 150-bilayer sample of the Fe^{3+}/Ni^{2+} grid network depicted in Fig. 1. Data are background corrected and shown for two sample orientations, parallel to the applied field and perpendicular to the applied field. The measuring field is 20 G in each case.

absorption fine structure analysis, infrared spectroscopy, and X-ray photoelectron spectroscopy [22,23]. The in-plane structure of the networks consists of a face-centered square grid of low spin Fe^{3+} ions that are bridged through cyanide to the second metal ions. For the Fe^{3+}/Ni^{2+} network, the in-plane lattice parameter is $a = 10.40$ Å [22], which yields a Fe–Ni separation of 5.2 Å. The corresponding cell edge for the Fe^{3+}/Mn^{2+} grid is 10.36 Å and that for the Fe^{3+}/Co^{2+} monolayer is 10.20 Å [23].

Magnetization measurements can be performed on films transferred onto Mylar. In the solid state, Fe^{3+}/Ni^{2+} mixed metal cyanides are ferromagnets, and a multilayered (150 bilayers) sample of the Fe^{3+}/Ni^{2+} network transferred off of the air/water interface undergoes a transition to a ferromagnetic state below $T_c \approx 8$ K, Fig. 2 [22,24,25]. The ordering temperature is lower than $T_c = 23$ K observed for the cubic analog, but is similar to other low-dimensional Fe–CN–Ni networks [11]. On the other hand, the real and imaginary components of the ac susceptibility (Fig. 3) show frequency

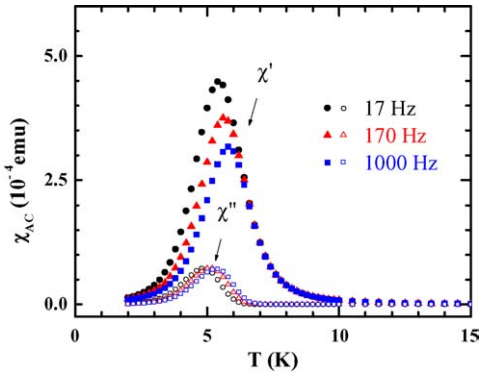

Fig. 3. Background corrected ac susceptibility for the 150-bilayer sample of the Fe^{3+}/Ni^{2+} square grid network at three frequencies. Data are acquired with the film parallel to the applied field with an ac field of 4 G.

dependence and are interpreted as being characteristic of spin-glass-type ordering of the ferromagnetic domains to form a cluster glass [25]. Domains are likely limited by structural coherence, the average of which is approximately 6 unit cell lengths, as determined from X-ray diffraction [22]. This value gives an average coherent particle size on the order of 3600 $Å^2$, which would contain approximately 144 ions (72 Fe^{3+} ions and 72 Ni^{2+} ions).

3. Monolayer, bilayer, multilayers

The magnetic data shown in Figs. 2 and 3 are for films of 150 bilayers. However, single-layer control over the deposition process provides an opportunity to observe how the magnetic properties of the system evolve as it changes from a monolayer to a bilayer to a multilayer film [25]. The network depicted in Fig. 1, can be transferred to solid supports in a controlled fashion, and if the dipping cycle begins with the substrate submerged in the water subphase, withdrawing it results in transfer of a single monolayer of the Fe–CN–Ni network oriented such that the inorganic network is in direct contact with the substrate surface (Fig. 4). On the other hand, if the substrate begins above the water surface, one dipping cycle of passing into the subphase and back out results in a bilayer (Fig. 4), with the organic portion of the material in contact with the substrate and the inorganic networks face-to-face, sandwiched in the center of the bilayer. The nature of the bonding interaction in the polar region between the networks is uncertain, but likely contains a mixture of covalent bonding via coordination of the axial cyanide of the iron complex to Ni^{2+} ions in the adjacent layer and hydrogen bonding via intercalated water molecules, giving an average distance between inorganic networks within the bilayer on the order of 10 Å or less. Finally, if the dipping cycle is repeated, multilayer films result with each bilayer of the Fe–CN–Ni network deposited onto the previous bilayer with alternating regions of organic-to-organic and inorganic-to-inorganic contacts (Fig. 4).

The frequency dependent $\chi_{ac}(T)$ data for the monolayer and bilayer samples are shown in Figs. 5 and 6 [25]. The presence of a $\chi''(T)$ component indicates uncompensated moments in the monolayer film, even though the peak has not clearly formed above $T = 2$ K. The $\chi'(T)$ clearly shows a frequency dependence, which again is indicative of spin-glass-like behavior and the peak position at all frequencies is below that of the multilayer film. Fitting the data to the Arrhenius equation:

$$\ln(\tau/\tau_0) = [E_a/(k_B T)], \quad (1)$$

where τ is the average relaxation time corresponding to the frequency of the ac measurement, and E_a/k_B the energy barrier to magnetic reversal in an isolated particle, yields $1 \times 10^{-15} < \tau_0 < 1 \times 10^{-13}$ s and $E_a/k_B = 70 \pm 5$ K. This value of τ_0 is below the range of $1 \times 10^{-11} < \tau_0 < 1 \times 10^{-9}$ s

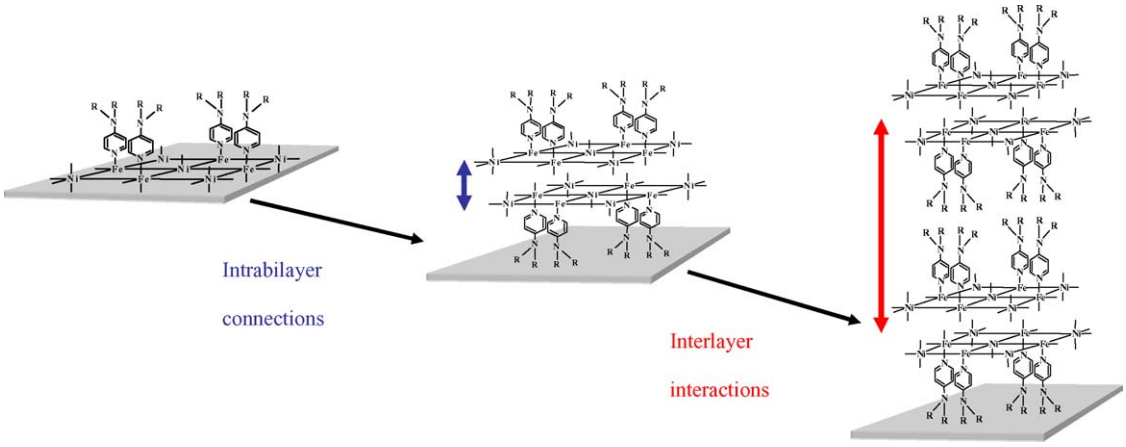

Fig. 4. The two-dimensional cyanide bridged Fe^{3+}/Ni^{2+} square grid networks assembled at the air-water interface can be transferred using the Langmuir–Blodgett technique as monolayer, bilayer, and multiple bilayer (multilayer) films. The different magnetic responses of the three films are attributed to differences in the in-plane, inter-plane, and long-range dipolar exchange interactions present in each sample architecture.

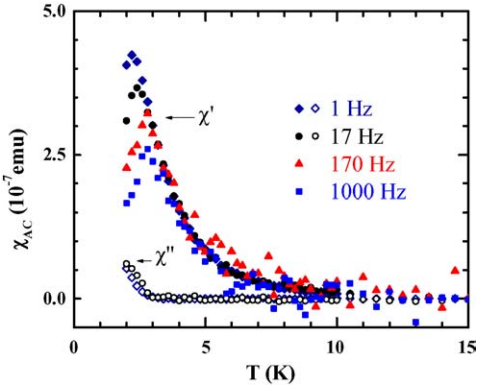

Fig. 5. The background corrected ac susceptibility, $\chi'(T)$ and $\chi''(T)$, for a monolayer of the Fe^{3+}/Ni^{2+} square grid aligned parallel to the measuring field. The samples were measured at different frequencies with an ac field of 4 G under zero applied dc field.

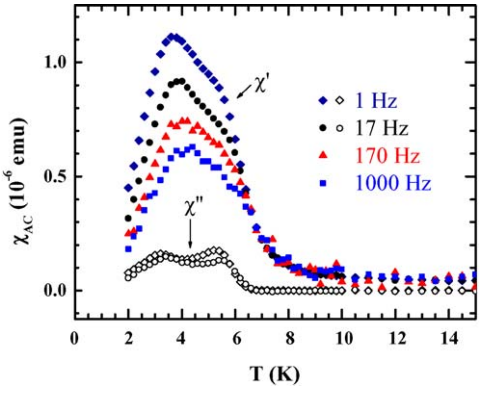

Fig. 6. The background corrected ac susceptibility, $\chi'(T)$ and $\chi''(T)$, for a bilayer sample of the Fe^{3+}/Ni^{2+} square grid aligned parallel to the measuring field. The samples were measured at different frequencies with an ac field of 4 G under zero applied dc field. The two processes observed in $\chi_{ac}(T)$ likely reflect sets of domains with different coherence lengths.

predicted for non-interacting ferromagnetic particles and indicates the presence of inter-particle interactions [26,27]. The strength of the interaction increases significantly as one progresses to the isolated bilayer and multilayer film for which $1 \times 10^{-19} < \tau_0 < 1 \times 10^{-21}$ s ($E_a/k_B = 170 \pm 10$ K) and $1 \times 10^{-29} < \tau_0 < 1 \times 10^{-31}$ s ($E_a/k_B = 350 \pm 5$ K), respectively. Therefore, the system may be best described as a progression from moderately interacting ferromagnetic domains in the monolayer to a more strongly interacting glass-like state, or cluster glass, in the bilayer and multilayer films.

Evidence for increasing interactions as bilayers and multilayers form is seen in other data, as well. The dc magnetization versus temperature plot of the multilayer sample, Fig. 2, shows significant anisotropy, with $M_{\parallel}$:$M_{\perp}$ of 3.4 at 2 K. The magnetic easy axis has a component parallel to the surface, reflecting the structural anisotropy of the film. The value of $M_{\parallel}$:$M_{\perp}$ is highest for the monolayer (ca. 22), and intermediate for the bilayer (4.6) [25], suggesting the presence of face-to-face coupling between layers in the bilayer that is not present in the monolayer, with additional interlayer interactions in the multilayer films. Similarly, the magnetic coercivity increases from monolayer to bilayer to multilayer (Fig. 7).

The changing interactions as the films are built from a monolayer to multiple-bilayers are summarized in Fig. 4. Additional layers add additional interactions, which are evident in the magnetic responses. The system may be described as a progression from moderately interacting ferromagnetic domains in the monolayer to a collective more strongly interacting glass-like state in the bilayer and multilayer films. The different magnetic responses of the three films are attributed to different in-plane, inter-plane, and long-range dipolar exchange interactions. This series shows that long-range magnetic dipolar interactions [28], across distances greater than 30 Å, can be important in supramolecular assemblies.

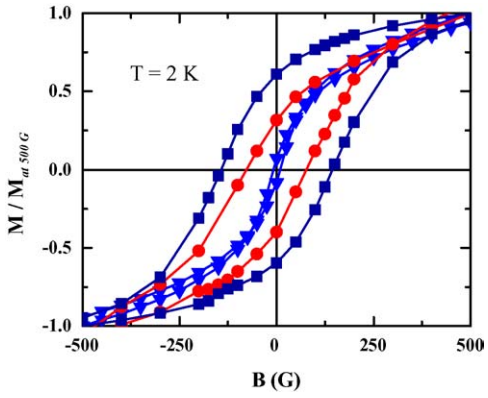

Fig. 7. Background corrected magnetization vs. field measured at 2 K for a monolayer (▼), bilayer (●), and multilayer (■) films of the Fe^{3+}/Ni^{2+} square grid aligned parallel to the applied field. (The total sweep width was −50 to 50 kG.) The lines are guides to the eye. The increasing coercivity reflects the larger number of exchange pathways upon building from monolayer to bilayer to multilayers.

4. Thin films of solid-state Prussian blue analogs

Many potential applications of magnetic cyanometallate bulk solids will also benefit if they can be processed as thin films. By far, the most studied route to cubic Prussian blue thin films is electrochemical deposition [29–32]. Other methods include adsorption onto sol–gel films [33], adsorption at Langmuir monolayers [34–37], and sequential deposition onto polyelectrolyte coated surfaces [38–40]. The morphologies of the deposited films vary, as the low solubility and poor crystallinity of most PB derivatives make surface wetting and the fabrication of continuous films difficult.

An alternative approach to cyanometallate thin films, shown in Fig. 8, is modeled after the layer-by-layer deposition process commonly used to for polyelectrolyte multilayers [41]. Thin films of the bulk solids are formed by sequential adsorption from solution of the appropriate metal ions and hexacyanometallate complexes. We modified the methods described by Millward et al. [38] and by Pyrasch and Tieke [39] by first derivatizing the surface with a monolayer of the two-dimensional iron–nickel–cyanide grid network [42,43], described earlier (Fig. 1). The two-dimensional grid network is essentially one layer of the Prussian blue structure and provides a surface layer with chemistry and structure that is similar to the cubic cyanometallates. Subsequent growth of the bulk phases is therefore continuous, completely covering the surface, even for very thin films. The Fe^{3+}/Ni^{2+} grid can be used as the primer layer for growing any of the mixed-metal Prussian blue analogs because its cell edge of 10.40 Å is in the middle of the range normally expected for the structurally similar bulk derivatives.

Thin films of several magnetic Prussian blue analogs prepared in this way have now been studied and shown to exhibit magnetic properties similar to the bulk materials [42,43]. Examples include $K_jFe_k[Fe(CN)_6]_l{\cdot}nH_2O$, $K_jNi_k[Fe(CN)_6]_l{\cdot}nH_2O$, $Cs_jNi_k[Cr(CN)_6]_l{\cdot}nH_2O$, $K_jCr_k[Cr(CN)_6]_l{\cdot}nH_2O$, and $Rb_jCo_k[Fe(CN)_6]_l{\cdot}nH_2O$. Film thicknesses range from a few nanometers to hundreds of nanometers.

5. Anisotropic photomagnetic effects in $Rb_jCo_k[Fe(CN)_6]_l{\cdot}nH_2O$

The Fe^{3+}/Co^{2+} Prussian Blue analogs, $M_jCo_k[Fe(CN)_6]_l{\cdot}nH_2O$, are known to be photomagnetic [19–21]. The

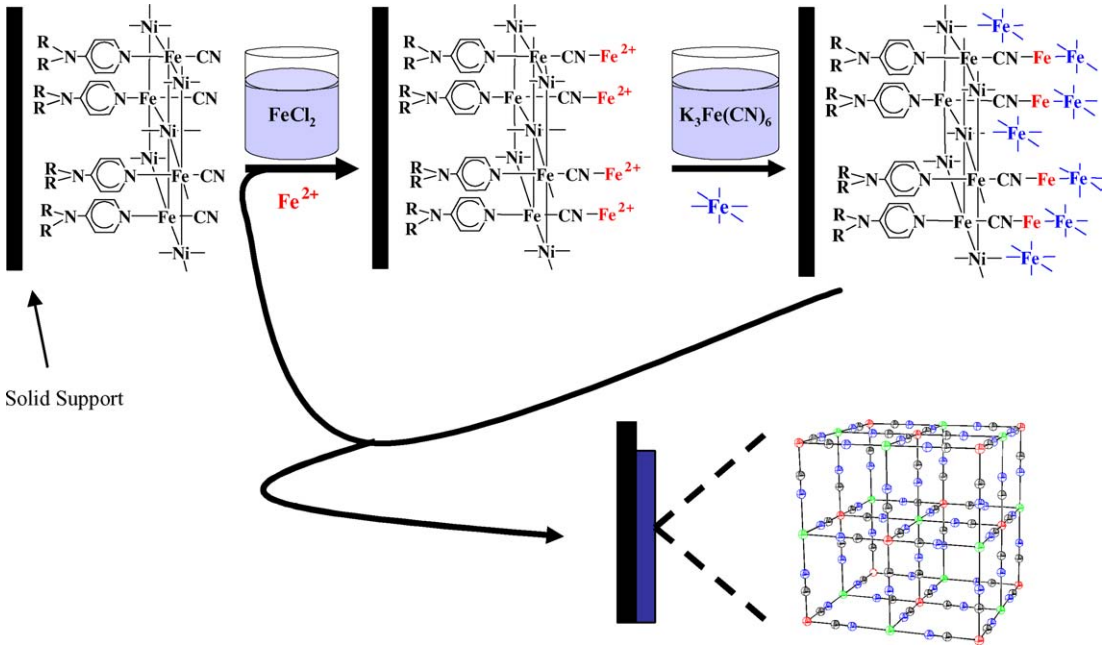

Fig. 8. The sequential deposition of cationic and anionic building blocks to form Prussian blue at a surface modified with a monolayer of a square grid template.

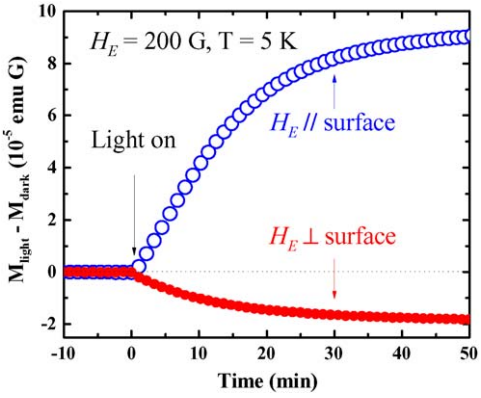

Fig. 9. The time dependence of the photoinduced magnetization of a film of $Rb_jCo_k[Fe(CN)_6]_l{\cdot}nH_2O$, prepared using the methods depicted in Fig. 8, when the external field is parallel and perpendicular to the plane of the film.

magnetization of the solids increases if irradiated in the ordered state with visible light. For certain compositions, the bulk compounds contain mixtures of two dominant spin configurations below T_c, a diamagnetic Fe^{2+}(LS, $S = 0$)–CN–Co^{3+}(LS, $S = 0$) state and a ferrimagnetic Fe^{3+}(LS, $S = 1/2$)–CN–Co^{2+}(HS, $S = 3/2$) state. The relative populations of each state can be tuned by changing the Fe/Co ratio of the sample [19,20]. Upon irradiation, electron transfer within the diamagnetic sites generates additional ferrimagnetic sites, increasing the samples magnetization. The photoinduced state is metastable, but can be maintained as long as the sample is kept below approximately 150 K.

Photomagnetic effects are also observed in $Rb_jCo_k[Fe(CN)_6]_l{\cdot}nH_2O$ thin films prepared by the sequential deposition methods, described above. However, the response of the interface-confined films is anisotropic [44]. The previously known increase in magnetization is observed with the magnetic field parallel to the film, but a *decrease* in magnetization is observed with the field perpendicular to the film. The time dependence of the photoinduced magnetism is shown in Fig. 9 for the two orientations upon field cooling the sample to 5 K in 200 G external field.

The anisotropic magneto-optical properties arise from interplay between the low-dimensional nature of the surface-confined film and the dipolar magnetic fields generated by the constant ferrimagnetic domains. When the sample is cooled from room temperature to below T_c, the ferrimagnetic and diamagnetic domains are randomly distributed. The primordial ferrimagnetic domains possess a net magnetic moment that aligns parallel to the external field (H_E). Consequently, diamagnetic domains adjacent to these sites experience the vector sum of the external field and a dipolar field (H_D) originating from the ferrimagnetic site. Importantly, H_D is antiparallel to H_E when the quasi-two-dimensional film is oriented perpendicular to the applied field, as illustrated in Fig. 10. When illuminated, the diamagnetic site will become ferrimagnetic, and the

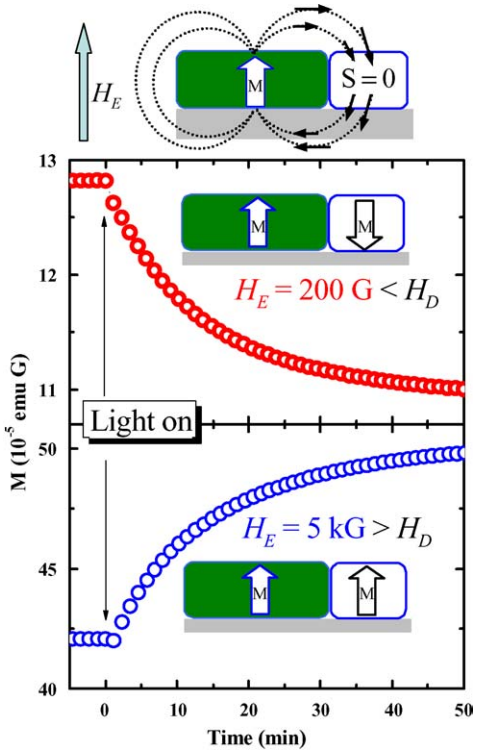

Fig. 10. The time dependence of the photoinduced magnetization at 2 K of a film of $Rb_jCo_k[Fe(CN)_6]_l{\cdot}nH_2O$ in the perpendicular orientation for two values of the external applied field, $H_E < H_D$ and $H_E > H_D$, and schematic illustrations of the spin configurations. The primordial ferrimagnetic domains are magnetized parallel to H_E, with neighboring diamagnetic domains ($S = 0$). The photoinduced magnetization of the diamagnetic domains depends on the vector sum of the external field, H_E, and the dipolar field of the ferrimagnetic domains, H_D. For $H_E < H_D$, the photoinduced moments result in a net decrease in magnetization. For $H_E > H_D$ the photoinduced moments give rise to a net increase in magnetization.

direction of the photoinduced magnetization will follow that of the net field. If H_D is larger that H_E, the total magnetization will decrease. On the other hand, if H_E is larger than H_D, the net photoinduced magnetization is expected to increase. This case is also observed experimentally with $H_E = 5$ kG, as shown in Fig. 10. When the plane of the film is parallel to the external field, H_D is also in the plane, and the powder-like in-plane distribution of orientations means that diamagnetic domains will experience some in-plane component, so the photoinduced moment results in an increase in total magnetization.

The dipolar field explanation for the anisotropic photomagnetic response depends on the quasi-two-dimensional nature of the film. If the film is too thick relative to the coherent domain size, then bulk properties should result. This point was explored experimentally by comparing films with different thickness and homogeneity [45]. All films exhibit the photo-induced increase in magnetization characteristic of $Rb_jCo_k[Fe(CN)_6]_l{\cdot}nH_2O$, but only quasi-two-dimensional smooth films with thickness on the order of 200 nm or less showed anisotropic response.

6. Summary

Cyanometallate networks generally form as insoluble polymers, presenting challenges to processing as homogeneous thin films. Synthesis directly at the site of interest can overcome difficulties associated with manipulating the preformed solids. This review has highlighted synthetic routes to films of metal cyanide networks that range from monomolecular layers to several hundred nanometers thick and prepared directly at interfaces. The thin film architectures and the methods of assembly combine to generate materials with new characteristics that the bulk solids do not possess. For example, single-layer control of the deposition process generates oriented samples, even though the structural coherence is small. In addition, the interface-assembled networks are inherently anisotropic, as exemplified by the orientation dependent photomagnetism of $Rb_jCo_k[Fe(CN)_6]_l{\cdot}nH_2O$.

Acknowledgements

Work described in this review was supported, in part, by the National Science Foundation through grants DMR-9900855 (DRT), DMR-0113714 (MWM and DRT), and DMR-0305371 (MWM), and by the Donors of the Petroleum Research Fund, administered by the ACS, ACS-PRF 36163-AC5 (MWM and DRT).

References

[1] V. Gadet, T. Mallah, I. Castro, M. Verdaguer, P. Veillet, J. Am. Chem. Soc. 114 (1992) 9213.
[2] T. Mallah, S. Thiebaut, M. Verdaguer, P. Veillet, Science 262 (1993) 1554.
[3] W.R. Entley, G.S. Girolami, Science 268 (1995) 397.
[4] M. Verdaguer, A. Bleuzen, V. Marvaud, J. Vaissermann, M. Seuleiman, C. Desplanches, A. Scuiller, C. Train, R. Garde, G. Gelly, C. Lomenech, I. Rosenman, P. Veillet, C. Cartier, F. Villain, Coord. Chem. Rev. 192 (1999) 1023.
[5] T. Mallah, C. Auberger, M. Verdaguer, P. Veillet, J. Chem. Soc., Chem. Commun. (1995) 61.
[6] A. Scuiller, T. Mallah, M. Verdaguer, A. Nivorozkhin, J.L. Tholence, P. Veillet, New J. Chem. 20 (1996) 1.
[7] R.J. Parker, L. Spiccia, K.J. Berry, G.D. Fallon, B. Moubaraki, K.S. Murray, Chem. Commun. (2001) 333.
[8] J. Larionova, M. Gross, M. Pilkington, H. Andres, H. Stoeckli-Evans, H.U. Gudel, S. Decurtins, Angew. Chem. Int. Ed. 39 (2000) 1605.
[9] M.P. Shores, J.J. Sokol, J.R. Long, J. Am. Chem. Soc. 124 (2002) 2279.
[10] P.A. Berseth, J.J. Sokol, M.P. Shores, J.L. Heinrich, J.R. Long, J. Am. Chem. Soc. 122 (2000) 9655.
[11] M. Ohba, H. Okawa, Coord. Chem. Rev. 198 (2000) 313.
[12] A. Marvilliers, S. Parsons, E. Riviere, J.P. Audiere, M. Kurmoo, T. Mallah, Eur. J. Inorg. Chem. (2001) 1287.
[13] H.Z. Kou, W.M. Bu, D.Z. Liao, Z.H. Jiang, S.P. Yan, Y.G. Fan, G.L. Wang, J. Chem. Soc., Dalton Trans. (1998) 4161.
[14] S.M. Holmes, G.S. Girolami, J. Am. Chem. Soc. 121 (1999) 5593.
[15] O. Hatlevik, W.E. Buschmann, J. Zhang, J.L. Manson, J.S. Miller, Adv. Mater. 11 (1999) 914.
[16] S. Ferlay, T. Mallah, R. Ouahes, P. Veillet, M. Verdaguer, Nature 378 (1995) 701.
[17] W.E. Buschmann, J.S. Miller, Inorg. Chem. 39 (2000) 2411.
[18] W.E. Buschmann, J. Ensling, P. Gutlich, J.S. Miller, Chem. Eur. J. 5 (1999) 3019.
[19] N. Shimamoto, S. Ohkoshi, O. Sato, K. Hashimoto, Inorg. Chem. 41 (2002) 678.
[20] V. Escax, A. Bleuzen, C.C.D. Moulin, F. Villain, A. Goujon, F. Varret, M. Verdaguer, J. Am. Chem. Soc. 123 (2001) 12536.
[21] O. Sato, T. Iyoda, A. Fujishima, K. Hashimoto, Science 272 (1996) 704.
[22] J.T. Culp, J.-H. Park, D. Stratakis, M.W. Meisel, D.R. Talham, J. Am. Chem. Soc. 124 (2002) 10083.
[23] J.T. Culp, J.-H. Park, M.W. Meisel, D.R. Talham, Polyhedron 22 (2003) 3059.
[24] J.-H. Park, J.T. Culp, D.W. Hall, D.R. Talham, M.W. Meisel, Physica B 329–333 (2003) 1152.
[25] J.T. Culp, J.-H. Park, M.W. Meisel, D.R. Talham, Inorg. Chem. 42 (2003) 2842.
[26] J.A. Mydosh, Spin Glasses, Taylor and Francis, Washington, DC, 1993.
[27] J.L. Dormann, D. Fiorani, E. Tronc, Adv. Chem. Phys. 98 (1997) 283.
[28] V. Laget, C. Hornick, P. Rabu, M. Drillon, R. Ziessel, Coord. Chem. Rev. 180 (1998) 1533.
[29] V.D. Neff, J. Electrochem. Soc. 125 (1978) 886.
[30] C.A. Lundgren, R.W. Murray, Inorg. Chem. 27 (1988) 933.
[31] O. Sato, T. Iyoda, A. Fujishima, K. Hashimoto, Science 271 (1996) 49.
[32] W.E. Buschmann, S.C. Paulson, C.M. Wynn, M.A. Girtu, A.J. Epstein, H.S. White, J.S. Miller, Chem. Mater. 10 (1998) 1386.
[33] Y.Z. Guo, A.R. Guadalupe, O. Resto, L.F. Fonseca, S.Z. Weisz, Chem. Mater. 11 (1999) 135.
[34] G.R. Torres, E. Dupart, C. Mingotaud, S. Ravaine, J. Phys. Chem. B 104 (2000) 9487.
[35] C. Lafuente, C. Mingotaud, P. Delhaes, Chem. Phys. Lett. 302 (1999) 523–527.
[36] C. Mingotaud, C. Lafuente, J. Amiell, P. Delhaes, Langmuir 15 (1999) 289.
[37] T. Yamamoto, Y. Umemura, O. Sato, Y. Einaga, Chem. Lett. 33 (2004) 500.
[38] R.C. Millward, C.E. Madden, I. Sutherland, R.J. Mortimer, S. Fletcher, F. Marken, Chem. Commun. (2001) 1994.
[39] M. Pyrasch, B. Tieke, Langmuir 17 (2001) 7706.
[40] A. Jaiswal, J. Colins, B. Agricole, P. Delhaes, S. Ravaine, J. Colloid Interface Sci. 261 (2003) 330–335.
[41] G. Decher, Science 277 (1997) 1232–1237.
[42] J.T. Culp, J.-H. Park, I.O. Benitez, M.W. Meisel, D.R. Talham, Chem. Mater. 15 (2003) 3431.
[43] J.T. Culp, J.-H. Park, I.O. Benitez, M.W. Meisel, D.R. Talham, Polyhedron 22 (2003) 2125.
[44] J.-H. Park, E. Cizmar, M.W. Meisel, Y.-D. Huh, F. Frye, S. Lane, D.R. Talham, Appl. Phys. Lett. 85 (2004) 3797.
[45] J.-H. Park, F. Frye, S. Lane, E. Cizmar, Y.-D. Huh, D.R. Talham, M.W. Meisel, Polyhedron, in press.